J Appl Electrochem
DOI 10.1007/s10800-008-9650-z

ORIGINAL PAPER

Oxygen reduction on Cu–Zn alloys

R. Procaccini · S. Ceré · M. Vázquez

Received: 1 April 2008 / Accepted: 1 August 2008

Abstract The reduction of oxygen on brass type Cu77Zn21Al2 in contact with 0.1 mol L^{-1} borax at pH 9.2 with and without chlorides was investigated and compared with the results on spectroscopic Cu. The surface film was characterized in situ by means of reflectance spectroscopy and by electrochemical impedance in the potential range negative to the open circuit potential. The main parameters associated to the kinetics of the oxygen reduction reaction were analyzed with a rotating disc electrode. The results show that within the potentials studied, a porous film was formed on brass while no significant spectral features were observed, except at −1.2 V where zinc oxo-hydroxides grow in chloride-free solutions and dissolve when chlorides are present in the system. The number of electrons exchanged for brass was close to 4 in both solutions, showing that oxygen is predominantly reduced to hydroxyl ions, with a reaction order equal to one. The residual presence of oxides on the surface results in Koutecky–Levich plots with slopes dependent on the applied potential and interfere with the calculation of the Tafel slope.

Keywords Surface films · Oxygen reduction · Copper alloys

1 Introduction

The impact of the oxygen reduction on fuel cells and materials degradation guarantees permanent interest in studying the mechanistic features. However, oxygen reduction on non-noble metals has not been extensively investigated. The various oxidation states typical of these elements can enter into catalytic cycles for the reduction of the important peroxide intermediate, as has been shown before for the reduction of H_2O_2 on copper and copper–nickel alloys [1]. In these cases, the presence of Cu(I) on the metal surface appears to be essential in the reduction mechanism. Thus, the passive film plays a key role in the mechanism of oxygen reduction reaction (ORR).

Many industrial types of equipment, particularly those related to aqueous solutions transport and heat exchange, are built from copper and copper-alloys. In these cases, where the metallic material is in contact with aqueous aerated electrolytes, the ORR constitutes the cathodic hemireaction of the corrosion process [2].

Within this framework, the effect of Zn as alloying element in brass was investigated, with emphasis on its incorporation to the surface film formed and the influence on the reaction kinetics.

The key parameters characterizing the kinetics of the oxygen reduction reaction were investigated. Also, the detrimental effect of the presence of chloride ions in the electrolyte was evaluated.

2 Experimental setup

The electrodes were constructed from spectroscopic grade copper (99.99%) and from aluminum–brass rods (77% Cu, 21% Zn, 2% Al; UNS 68700) provided by LCL Pty Ltd™, Australia. For the steady-state experiments, metal disks were conveniently mounted on PVC holders, including an electrical connection welded at the rear side. The rotating-disk electrodes were built embedding rods of Cu

R. Procaccini · S. Ceré · M. Vázquez (✉)
División Corrosión, INTEMA Facultad de Ingeniería,
Universidad Nacional de Mar del Plata (UNMdP),
Juan B. Justo 4302, B7608FDQ Mar del Plata, Argentina
e-mail: mvazquez@fi.mdp.edu.ar

and Cu–Zn alloys in Teflon™ cylindrical holders. The electrodes were abraded with a sequence of emery papers and finally mirror polished with 0.05 μm alumina powder.

A conventional three-electrode cell was used to carry out the electrochemical measurements. A Pt wire of large-enough area was used as auxiliary electrode. Two different electrodes were used as reference: $Hg/Hg_2SO_4/K_2SO_4$ 0.6 mol L^{-1} (0.616 V vs. NHE, labeled MME) for the electrochemical experiments and Ag/AgCl/NaCl 3 mol L^{-1} (0.208 V vs. NHE) when recording reflectance spectra. However, to simplify comparisons, all the potential values were indicated taking MME as reference. To control current and potential a Voltalab PGP 201 potentiostat was used.

Borax 0.1 mol L^{-1} (pH = 9.2) and borax 0.1 + 0.01 mol L^{-1} NaCl were used as electrolytes, as indicated. Both were deaerated for 15 min with high-purity N_2 prior to each measurement, except for the oxygen reduction polarization curves, where the electrolyte was saturated with O_2 during 15 min. The oxygen concentration in oxygen-saturated electrolytes was taken as 1.15×10^{-3} mol L^{-1} in borax solutions and 1.08×10^{-3} mol L^{-1} in borax containing 0.01 mol L^{-1} of Cl^- ions. These measurements were carried out using an oxygen meter PST3 attached to an optical fiber sensor. All the experiments were carried out at room temperature (20 ± 2°C).

To record cyclic voltammograms the electrodes were pretreated in both solutions by holding them at −1.6 V for 10 min to have a reproducible initial condition. Finally, 2.1 V were scanned, using a sweep rate of 0.01 V s^{-1}.

To investigate the kinetics of the oxygen reduction reaction, polarization curves were registered at 0.02 V s^{-1} using five different rotation rates between 225 and 1,600 rpm. The rotating disk experiments were carried out using a Radiometer™ controller (CTV101). The electrodes were pretreated by holding them at −1.6 V in the deaerated electrolyte during 15 min. Then, the electrolyte was saturated with oxygen, bubbling the gas for at least 15 min prior to recording the polarization curves.

Electrochemical impedance spectroscopy (EIS) tests were performed at pre-reduced electrodes held at −1.6 V and then pre-oxidized at −0.9 V for 15 min. The solution was used without stirring and saturated with oxygen. The AC voltage signal amplitude is ±0.01 V_{rms} and the frequency was varied between 100 kHz and 1 mHz. The results were analyzed using equivalent circuits. The experimental data were fitted to the proposed equivalent circuit using ZView [3].

The composition of the surface films was evaluated by means of reflectance spectroscopy [4]. The absorption spectra were recorded in-situ. The baseline was corrected by polarizing two identical polished surfaces at −1.4 V. The spectrum of each surface was recorded after holding the electrodes at a potential range between −1.4 and −0.5 V for a certain period of time in oxygen saturated electrolyte. The spectroelectrochemical measurements were carried out using a commercial double-beam spectrophotometer (Shimadzu UV 160 A), conveniently modified as described elsewhere [5].

3 Results and discussion

3.1 Characterization of the surfaces by cyclic voltammetry

The cyclic voltammograms of copper in deaerated borax pH 9.2 with and without chloride ions are presented in Fig. 1. Without chloride ions presents, two broad anodic peaks appeared at −0.4 V (Cu_2O formation) and at 0.15 V (CuO formation), while the two cathodic peaks were located at −0.75 V (CuO reduction to Cu_2O) and −1.0 V (Cu_2O reduction). When the electrolyte contained 0.01 mol L^{-1} of Cl^-, a new anodic peak at −0.55 V is probably due to a copper–chloride species and three reduction peaks were now registered. The most positive of them, at −0.62 V, may correspond to CuO reduction, the next at −0.68 V can be attributed to a copper–chloride species (probably "atacamite": $Cu_2(OH)_3Cl$ [6]), and the most negative CV peak at −1.0 V can be assigned to Cu_2O reduction.

For the sake of comparison, the cyclic voltammogram of brass is presented in Fig. 2, recorded in the same conditions as those shown for copper in Fig. 1. In borax, a broad anodic peak appeared at −1.2 V (most likely due to a Zn containing specie), another one at −0.4 V (Cu_2O formation), while a plateau started at −0.2 V (CuO formation). The cathodic peaks can be seen at −0.7 V (CuO reduction to Cu_2O) and −1.1 V (Cu_2O reduction). A third cathodic peak at −1.35 V

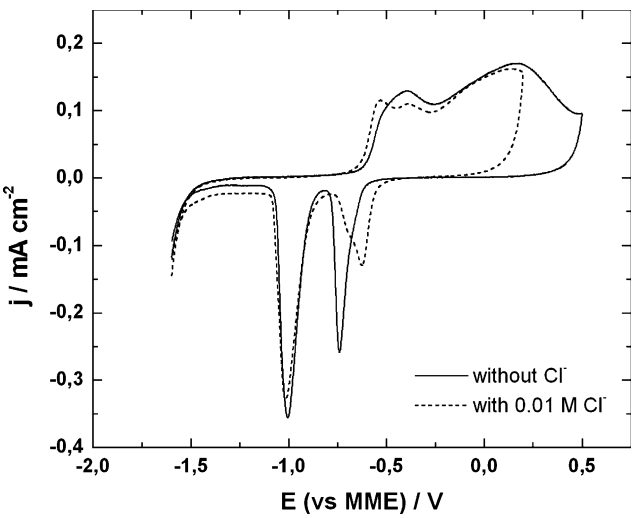

Fig. 1 Voltammograms of Cu electrodes in contact with deaerated 0.1 mol L^{-1} borax, with and without 0.01 mol L^{-1} NaCl (v = 0.01 V s^{-1})

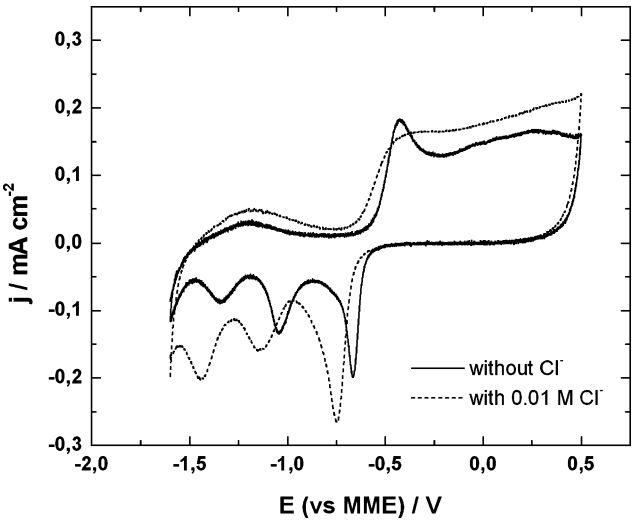

Fig. 2 Voltammograms of brass electrodes in contact with deaerated 0.1 mol L^{-1} borax, with and without 0.01 mol L^{-1} NaCl ($v = 0.01$ V s^{-1})

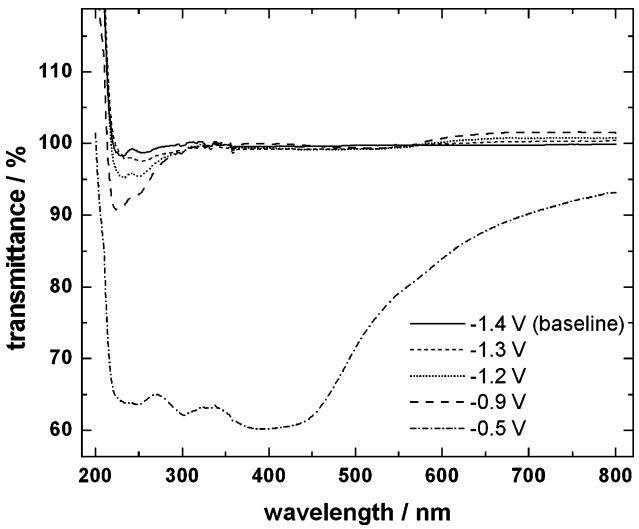

Fig. 3 Differential reflectance spectra for brass in oxygen saturated borax solution, after holding the electrode at −1.3, −1.2, −0.9 and −0.5 V for 10 min

was probably due to $HCuO_2^-$ reduction [7, 8]. When chloride ions were incorporated to the solution, the same anodic peaks as for brass in borax could be observed but there is a negative shift in the position of the peaks.

3.2 Characterization by reflectance spectroscopy

Figure 3 presents reflectance spectra recorded while performing a cathodic scan on brass in borax 0.1 mol L^{-1} at −1.3, −1.2, −0.9 and −0.5 V (holding the potential for 10 min at each value). At potentials negative to −0.6 V no significant spectral characteristics were observed, except at

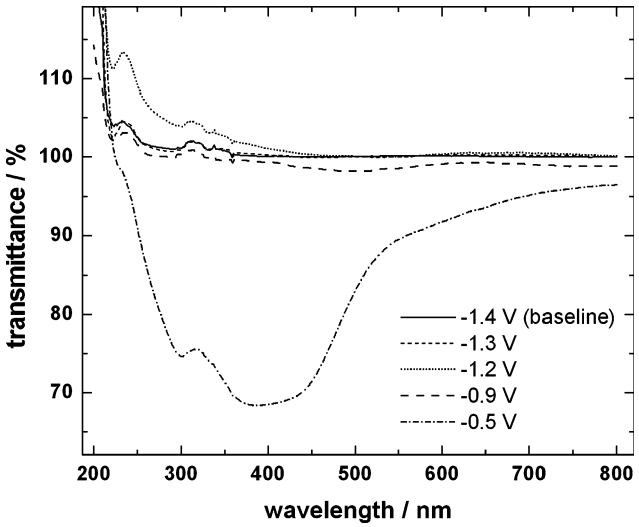

Fig. 4 Differential reflectance spectra for brass in oxygen saturated borax solution containing 0.01 mol L^{-1} NaCl, after holding the electrode at −1.3, −1.2, −0.9 and −0.5 V for 10 min

−1.2 V when zinc oxo-hydroxides grow in agreement with the results of the cyclic voltammetry (Fig. 2). The main spectral characteristic for zinc is a peak located at 230–250 nm. When the potential scan moved towards values more positive than −0.6 V, the main spectral features corresponded to those for Cu_2O: a broad peak at 462 nm, a lower one at 240 and 360–380 nm, and a shoulder at 237 nm [4, 5, 9]. The presence of CuO in the film was evidenced by a featureless absorption band, increasing in intensity at wavelengths shorten than 280 nm. For this reason, CuO identification just from reflectance spectra tends to be difficult. All these same results were found for copper in borax 0.1 mol L^{-1}.

When chloride ions were added to the electrolyte, some changes in the spectra were observed, as shown in Fig. 4. When chloride ions were present, mainly copper features were observed as the potential scan moved towards −0.6 V. However, at −1.2 V an increase in transmittance at short wavelengths could be observed, which was attributed to zinc oxo-hydroxides dissolution. This was in agreement with previous results published by Kim and col. [9] where they had observed dezincification following the decrease in absorbance at about 320 nm (correlated to an increase in transmittance, in our case). This was also confirmed by independent experiments, where a decrease in the charge of a cathodic peak at −1.2 V was registered during voltammograms performed under rotation.

3.3 Characterization by electrochemical impedance spectroscopy

The results of the impedance spectra recorded on brass are shown in Fig. 5. The effect of the presence of chloride is

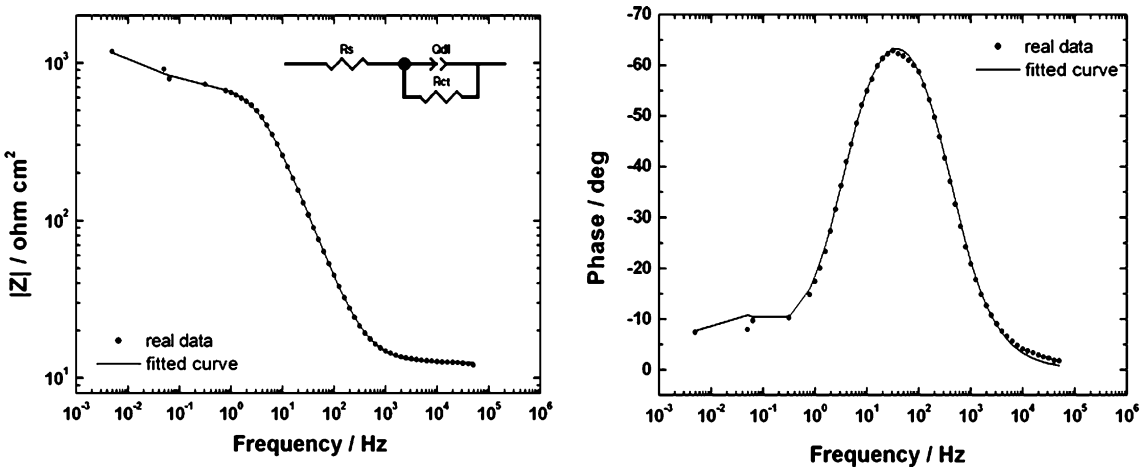

Fig. 5 Impedance spectra recorded on brass electrodes held at −0.9 V in oxygen saturated borax solution. The symbols represent the data and the lines the fitting results. The equivalent circuit employed is also shown

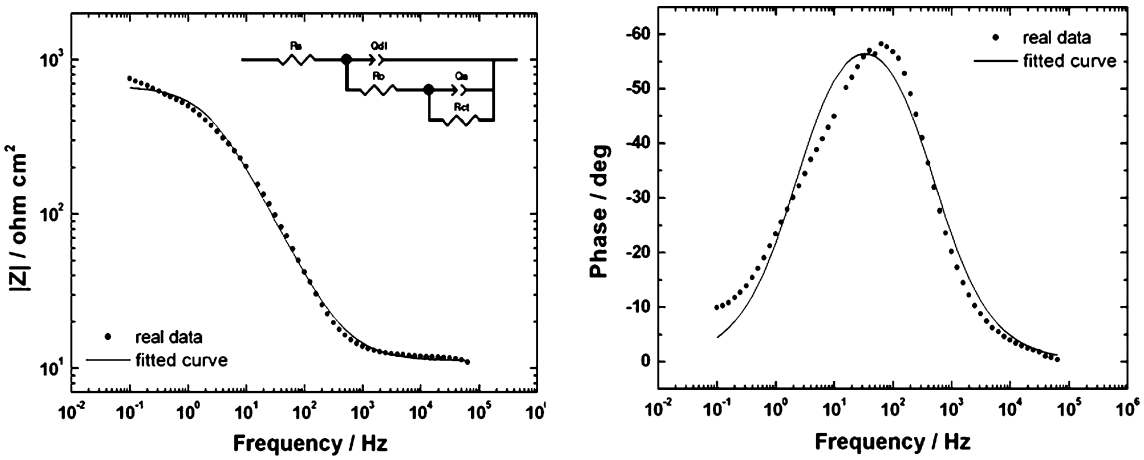

Fig. 6 Impedance spectra recorded on brass electrodes held at −0.9 V in oxygen saturated borax solution containing 0.01 mol L^{-1} NaCl. The symbols represent the data and the lines the fitting results. The equivalent circuit employed is also shown

presented in Fig. 6. Both groups of experiments were carried out at −0.9 V after pre-reducing the electrodes at −1.6 V during 15 min.

EIS data fit results are also shown in Figs. 5 and 6, together with the respective equivalent circuits used. The experimental data are considered to be sufficiently well fitted by the proposed circuits. Table 1 presents the optimised values for the various parameters involved. For copper, the impedance results were different from those obtained for brass, and Table 1 shows data fit results for comparison. A conventional Randles circuit, where a constant phase element (CPE) was used instead of the capacitor, gave satisfactory fits for experiments carried out at −0.9 V for copper. Surface roughness, insufficient polishing, grain boundaries and surface impurities have been mentioned among the main reasons allowing the use of CPEs in equivalent circuits of corroding electrodes [10]. The impedance of CPEs can be written as:

$$Z_{CPE} = [Q(j\omega)^n]^{-1} \quad (1)$$

where Q is the frequency-independent constant or pseudo-capacitance and n a constant power, with $-1 < n < 1$. A rough or porous surface can cause a double layer capacitance to appear as a constant phase element with n between 0.5 and 1.

On the other hand, for brass, a more complex circuit with two time constants was used. This is in agreement with the anodic peak observed between −1.4 and −0.8 V for brass (Fig. 2) and the reflectance spectra for brass at −0.9 V (Figs. 3 and 4). This circuit is typical of a duplex film composed of mostly porous oxides and has been used before in similar systems [11–13]. In contrast, the data recorded on copper can be interpreted by means of a simple Randles-type circuit.

Care should be taken with the data analysis when different models are applied. Still, it is important to note that the total

Table 1 Optimized values for the parameters employed in fitting the data in Figs. 5 and 6 to the equivalent circuit proposed

Electrode/solution	Element	Value	% Error
Cu without Cl^-	Rs/Ω·cm^2	15.94	0.57
	Qdl/Ω^{-1}·cm^{-2}·s^n	4.43 × 10^{-5}	1.75
	n	0.92	0.32
	Rct/Ω·cm^2	987	1.07
Cu 0.01 M Cl^-	Rs/Ω·cm^2	15	1.32
	Qdl/Ω^{-1}·cm^{-2}·s^n	4.59 × 10^{-5}	4.76
	n	0.88	0.82
	Rct/Ω·cm^2	462.9	1.55
Brass without Cl^-	Rs/Ω·cm^2	12.51	0.36
	Qdl/Ω^{-1}·cm^{-2}·s^n	9.72 × 10^{-5}	1.26
	n	0.86	0.24
	Ro/Ω·cm^2	716	0.96
	Qa/Ω^{-1}·cm^{-2}·s^n	1.014 × 10^{-2}	9.85
	n	0.73	6.23
	Rct/Ω·cm^2	568.7	7.89
Brass 0.01 M Cl^-	Rs/Ω·cm^2	11.79	0.47
	Qdl/Ω^{-1}·cm^{-2}·s^n	8.81 × 10^{-5}	5.12
	n	0.88	0.77
	Ro/Ω·cm^2	270.6	10.5
	Qa/Ω^{-1}·cm^{-2}·s^n	6.89 × 10^{-4}	7.21
	n	0.58	6.52
	Rct/Ω·cm^2	535.7	8.27

resistance for brass was always higher than that for copper. This showed the effect of the film formed on the surface and justified the higher corrosion resistance for brass in both electrolytes when compared with copper. It could be also observed that Ro for brass, associated to the resistance within the pores, presented a lower value when chlorides were present in the electrolyte, showing a less protective film.

3.4 Cathodic polarization curves

Cathodic polarization curves were registered on previously reduced surfaces using rotating disk electrodes, as described above. The potential scan started at −1.6 V and was interrupted at least 0.2 V negative to the open circuit potential in order to prevent undesired oxide formation. A typical result for brass in borax 0.1 mol L^{-1} with and without chloride ions is presented in Fig. 7. Two distinctive regions could be distinguished: a potential range of mixed control (activated and diffusional), where current and potential were interdependent and a diffusional range at more negative potentials, where a limiting current was achieved. On copper, the current density decreased in the mixed control region when Cl^- ions were present (not

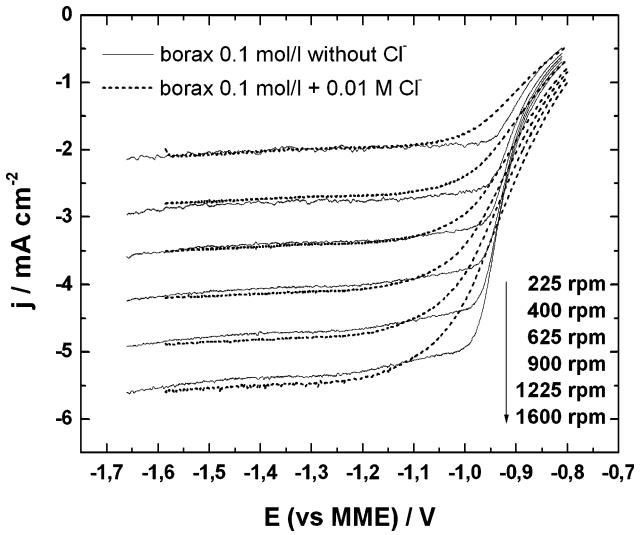

Fig. 7 RDE polarization curves for brass electrodes pre-reduced at −1.4 V during 15 min in oxygen saturated borax solution with and without chloride ions. Scan rate: 0.01 mV s^{-1}

showed). Similar results were found by Vazquez et al. [1, 2] for oxygen and peroxide reduction on copper in presence of chloride ions. This was attributed to the presence of CuO inhibiting oxygen reduction, which can be dissolved in the presence of chloride ions.

The number of electrons exchanged in the cathodic hemireaction could be calculated from the slope of the appropriated representation of the Levich equation [14]:

$$j_L = 0.20nFD^{2/3}v^{-1/6}C_B\omega^{1/2} \quad (2)$$

where j_L was the limiting current density in A cm^{-2}, D the diffusion coefficient of the electroactive species (1.9 × 10^{-5} cm^2 s^{-1}), v was the kinematic viscosity (0.01 cm^2 s^{-1}), C_B represented the oxygen concentration in the bulk solution (1.15 × 10^{-3} mol L^{-1} in borax solutions and 1.08 × 10^{-3} mol L^{-1} in borax containing 0.01 mol L^{-1} of Cl^- ions), and ω was the rotation rate in rpm.

Levich representations are shown in Figs. 8 and 9 for brass without and with chloride ions present, respectively. The data calculated from these plots are shown in Table 2. The linear dependence of the current density on $\omega^{1/2}$ was indicative of a diffusion-limited process according to the Levich equation. For both brass and copper, the overall number of electrons exchanged in the oxygen reduction reaction on pre-reduced surfaces was slightly lower than 4 [1, 15] Table 3.

Two possible routes exist for the electrochemical reduction of oxygen, a sequential and a direct pathway [16, 17]. The difference lays is in the generation of peroxide as intermediate, which occurs in the first case. The general mechanism can be schematically represented as [18]

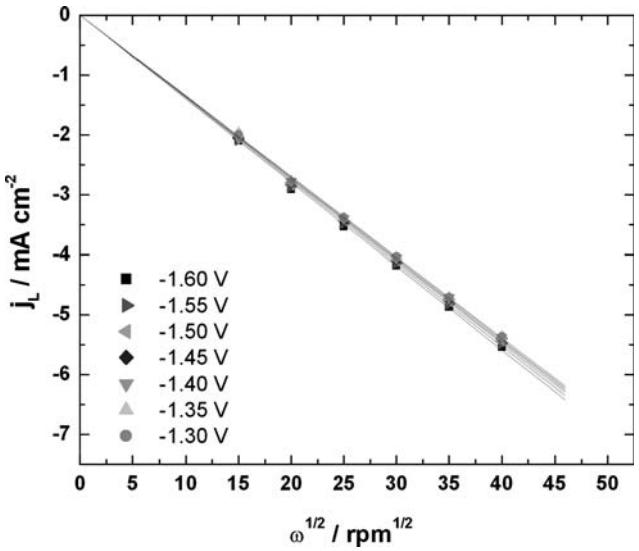

Fig. 8 Levich plots of brass electrodes in contact with 0.1 mol L^{-1} borax solution

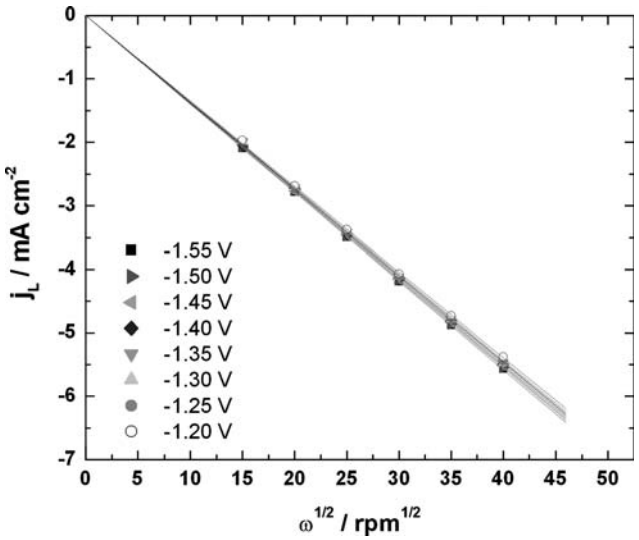

Fig. 9 Levich plots of brass electrodes in contact with 0.1 mol L^{-1} borax solution containing 0.01 mol L^{-1} NaCl

Table 2 Levich plots for brass in borax 0.1 mol L^{-1} solution

Expriment	e^- number
Levich	
Brass without Cl^- ions	3.75 ± 0.05
Brass with 0.01 M Cl^- ions	3.88 ± 0.05

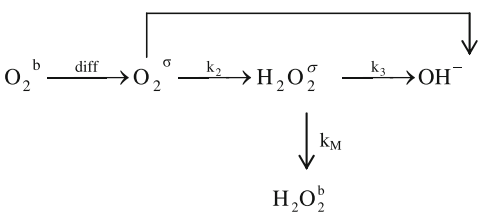

(I)

Table 3 Tafel slopes for brass in borax 0.1 mol L^{-1} solution. (I), (II) and (III) corresponds to plots showed in Fig. 13

Experiment	Tafel ope/V dec^{-1}
Brass without Cl^- ions (higher potentials)	0.069 ± 0.007 (I)
Brass without Cl^- ions (lower potentials)	0.228 ± 0.027 (II)
Brass with 0.01 M Cl^- ions	0.206 ± 0.0 18 (III)

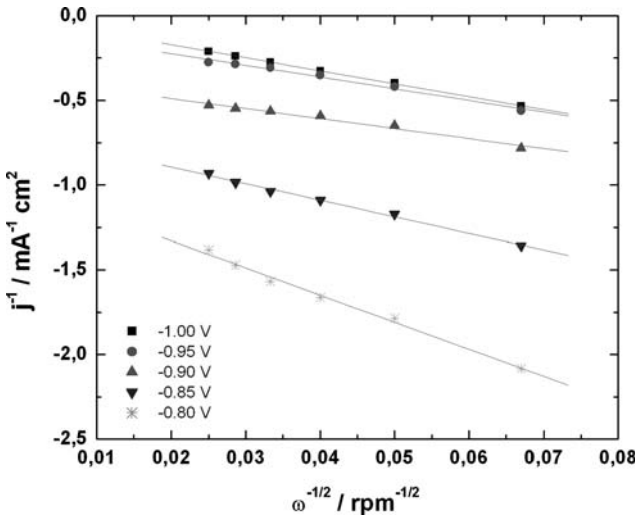

Fig. 10 Koutecky–Levich plots of brass electrodes in contact with 0.1 mol L^{-1} borax solution

Less than four electrons being exchanged clearly show that there is a bifurcation point in the reduction sequence (I) with a subsequent loss of peroxide into the solution. A "direct" reduction mechanism must involve a breakage of the O–O bond at the rate determining step. It could be proposed that the competing reactions responsible for the bifurcation was the μ-peroxo bridge adsorption of O_2 in vicinal Cu(0) sites, in competition with an end-on superoxide adsorption, the latter leading to the loss of some peroxide in the solution.

In the mixed controlled range of the polarization curves, the Koutecky–Levich equation (Eq. 3) can be used [11]:

$$\frac{1}{j} = \frac{1}{j_A} + \frac{1}{0.20nFD_R^{2/3}\nu^{-1/6}C_R^*\omega^{1/2}} \quad (3)$$

where the symbols have the same meaning as those used in Eq. 2.

The number of electrons exchanged as a function of the applied potential, could be calculated from the slope of the j^{-1} vs $\omega^{-1/2}$ representation. This equation should be used carefully, because it is written assuming that reaction order is 1 for the studied species. In this case, plotting log |j| vs log $[1 - (j / j_L)]$ the reaction order for oxygen was confirmed (not shown). Figures 10 and 11 show the Koutecky–Levich plots obtained for brass with and without chloride ions, where it could be seen that the slope of the lines

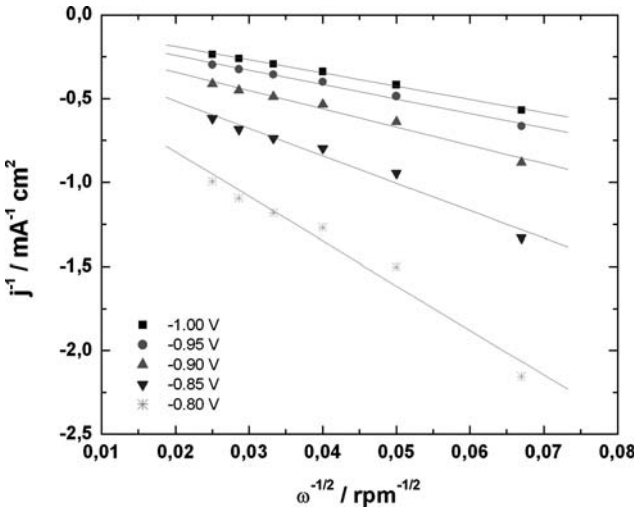

Fig. 11 Koutecky–Levich plots of brass electrodes in contact with 0.1 mol L^{-1} borax solution containing 0.01 mol L^{-1} NaCl

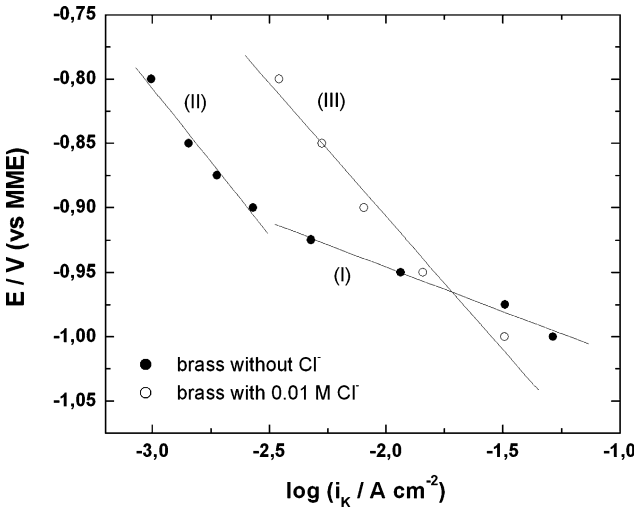

Fig. 13 Tafel plots for brass in borax 0.1 mol L^{-1} solution, with and without 0.01 mol L^{-1} NaCl

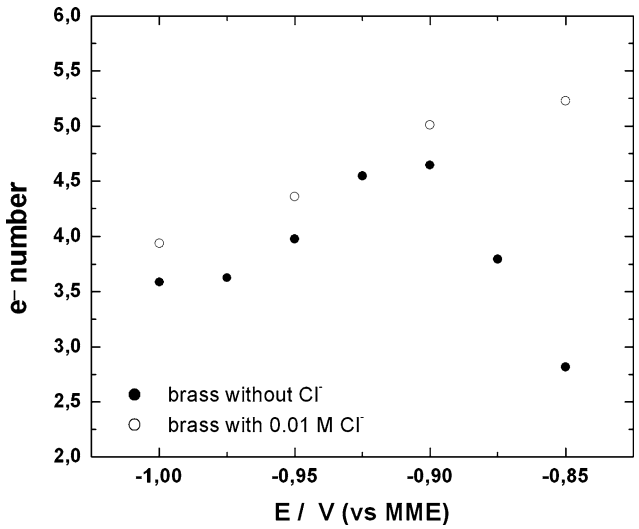

Fig. 12 Electrons exchanged plotted against potential for brass in borax 0.1 mol L^{-1} solution, with and without 0.01 mol L^{-1} NaCl

changed with potential. The number of electrons, calculated from Eq. 3 at each potential value is represented in Fig. 12. In the case of brass, the maximum in the curves (with $n > 4$) could be explained by the simultaneous reduction of residual oxides.

The Tafel slopes could be calculated extrapolating the kinetic current density from the measured currents to infinite rotation rate from the plots in Figs. 10 and 11. A representation of log i_k as a function of potential for brass in both solutions is shown in Fig. 13. When no chlorides were present in the solution, the data seemed to adjust to two different slopes, probably reflecting how the composition of the surface films depended on potential. In the presence of chlorides this situation was partially attenuated by chemical dissolution and a slope of -206 mV dec^{-1} could be calculated. Large values as this one were reported before and attributed to O_2 reduction occurring on a surface which is never oxide-free. The composition of the surface layer depended on the electrode pre-treatment, the presence of oxygen as chemical oxidant and the presence of chlorides as complexing agents for Cu(I) and Cu(II) species [19–21].

4 Conclusions

Within the potential range studied a porous film was formed onto brass which contained some zinc oxo-hydroxides. These species were not present when chlorides were incorporated to the system due to the solubility of the Zn species.

The maximum number of electrons exchanged during the oxygen reduction reaction on brass was close to 4 in both solutions, meaning that oxygen is predominantly reduced to hydroxide, while the oxygen reduction reaction order was one. Residual surface oxides were surely involved in a complex mechanism and were also responsible for Tafel slope values that deviated from the expected 0.12 V/dec

Acknowledgements The authors acknowledge the financial support received from the National Research Council of Argentina, CONICET and from the Universidad Nacional de Mar del Plata.

References

1. Vázquez MV, de Sánchez SR, Calvo EJ, Schiffrin DJ (1994) J Electroanal Chem 374:179

2. Calvo EJ, Schiffrin DJ (1988) J Electroanal Chem 243:171
3. ZPlot for Windows, ver. 3.0 (2007) Scribner Associates Inc., NC
4. Hummel RE (1983) Phys Stat Sol (a) 76:11
5. de Sánchez SR, Berlouis LEA, Schiffrin DJ (1991) J Electroanal Chem 307:73
6. Bianchi G, Longhi P (1973) Corros Sci 13:853
7. Gennero de Chialvo MR, Marchiano SL, Arvia AJ (1984) J Appl Electrochem 16:165
8. Milosev I, Strehblow H-H (2003) J Electrochem Soc 150:B517
9. Kim B-S, Piao T, Hoier SN, Park S-M (1995) Corros Sci 37:557
10. Aljinovic LJ, Gudic S, Smith M (2000) J Appl Electrochem 30:973
11. Brizuela F, Procaccini R, Ceré S, Vázquez MV (2006) J Appl Electrochem 36:583
12. Bard AJ, Faulkner LR (1980) Electrochemical methods fundamentals and applications. Wiley, NY
13. Mansfeld F (1988) Corrosion 44:856
14. Ismail KM, Elsherif RM, Badaway WA (2005) Corrosion 61:411
15. Vazquez MV, de Sánchez SR, Calvo EJ, Schiffrin DJ (1994) J Electroanal Chem 374:189
16. Tarasevich MR, Sadkowski A, Yeager EB. In: Conway BE, Mockis JO'M, Yeager EB, Khan S, White R (ed) Comprehensive treatise of electrochemistry. Plenum Press, NY
17. Pleskov YV, Filinovskii VY (1976) The rotating disc electrode. Consultants Bureau, NY
18. Wroblowa HS, Pan YC, Razumney G (1976) J Electroanal Chem 69:195
19. Ceré S, Vázquez MV, de Sánchez SR, Schiffrin DJ (2001) J Electoanal Chem 505:118
20. King F, Quinn MJ, Litke CD (1995) J Electroanal Chem 385:45
21. Zagal JH, Aguirrea MJ, Páez MA (1998) J Electroanal Chem 437:45